# Matrix morphogenesis in cornea is mediated by the modification of keratan sulfate by GlcNAc 6-*O*-sulfotransferase

Yasutaka Hayashida*, Tomoya O. Akama†, Nicola Beecher‡, Philip Lewis‡, Robert D. Young‡, Keith M. Meek‡, Briedgeen Kerr§, Clare E. Hughes§, Bruce Caterson§, Akira Tanigami¶, Jun Nakayama‖, Michiko N. Fukada†, Yasuo Tano*, Kohji Nishida**††, and Andrew J. Quantock‡

*Department of Ophthalmology, Osaka University Medical School, 2-2 Yamadaoka, Suita, Osaka 565-0871, Japan; †Glycobiology Program, Burnham Institute for Medical Research, 10901 North Torrey Pines Road, La Jolla, CA 92037; ‡Structural Biophysics Group, School of Optometry and Vision Sciences, Cardiff University, Redwood Building, Cathays Park, Cardiff CF10 3NB, United Kingdom; §Connective Tissue Biology Laboratory, School of Biosciences, Cardiff University, Museum Avenue, Cathays Park, Cardiff CF10 3US, United Kingdom; ¶Otsuka GEN Research Institute, Otsuka Pharmaceutical Co. Ltd., Tokushima 771-0192, Japan; ‖Department of Pathology, Shinshu University School of Medicine, Matsumoto 390-8621, Japan; and **Department of Ophthalmology, Tohoku University Medical School, 1-1 Seiryo-cho, Aobaku, Sendai, Miyagi 980-8574, Japan

Edited by Stuart A. Kornfeld, Washington University School of Medicine, St. Louis, MO, and approved July 12, 2006 (received for review June 29, 2006)

**Matrix assembly and homeostasis in collagen-rich tissues are mediated by interactions with proteoglycans (PGs) substituted with sulfated glycosaminoglycans (GAGs). The major GAG in cornea is keratan sulfate (KS), which is N-linked to one of three PG core proteins. To ascertain the importance of the carbohydrate chain sulfation step in KS functionality, we generated a strain of mice with a targeted gene deletion in *Chst5*, which encodes an *N*-acetylglucosamine-6-*O*-sulfotransferase that is integral to the sulfation of KS chains. Corneas of homozygous mutants were significantly thinner than those of WT or heterozygous mice. They lacked high-sulfated KS, but contained the core protein of the major corneal KSPG, lumican. Histochemically stained KSPGs coassociated with fibrillar collagen in WT corneas, but were not identified in the *Chst5*-null tissue. Conversely, abnormally large chondroitin sulfate/dermatan sulfate PG complexes were abundant throughout the *Chst5*-deficient cornea, indicating an alteration of controlled PG production in the mutant cornea. The corneal stroma of the *Chst5*-null mouse exhibited widespread structural alterations in collagen fibrillar architecture, including decreased interfibrillar spacing and a more spatially disorganized collagen array. The enzymatic sulfation of KS GAG chains is thus identified as a key requirement for PG biosynthesis and collagen matrix organization.**

collagen | glycosaminoglycans | proteoglycans

Glycosaminoglycans (GAGs) substituted on proteoglycans (PGs) are influential in defining collagen fibrillar architecture in a wide range of connective tissue matrices. Keratan sulfate (KS) is an important constituent of several collagen-rich tissues and is the major GAG in cornea where it is N-linked to asparagine residues in one of three PG core proteins: lumican (1), keratocan (2), and mimecan/osteoglycin (3). Human corneal GlcNAc 6-*O*-sulfotransferase (also known as human GlcNAc6ST-5 and GST4$\beta$) is the responsible enzyme for the synthesis of high-sulfated KS via the transfer of sulfate onto the GlcNAc 6-*O* position of the KS backbone (4).

Fairly compelling evidence exists for a regulatory role for KSPGs in the maintenance of corneal matrix structure in a number of species. The avian cornea *in ovo*, for example, synthesizes an unsulfated form of KS midway through development when it is structurally disorganized and transmits relatively little light, but switches to produce a sulfated KS GAG as it becomes transparent and attains a more well ordered collagen fibrillar ultrastructure (5, 6). KS sulfation patterns are also altered in opaque, structurally disorganized corneal scar tissue in rabbits (7, 8) and in cloudy human corneas with the inherited disease, macular corneal dystrophy (9), which is caused by mutations in *CHST6*, a gene encoding human corneal GlcNAc 6-*O*-sulfotransferase (10).

Hybrid type I/V collagen fibrils are the cornea's main nonspecular light-scattering elements and are formed into wide, interweaving belts or lamellae that lie approximately in the tissue plane (11). Within each lamella the fibrils are regularly spaced and have remarkably uniform diameters. It is this configuration that sets the cornea apart from other collagenous (and opaque) connective tissues and is responsible for its transmission of visible light (12). KSPGs are believed to shape the architecture of the cornea via interactions with fibrillar collagen.

Investigations of the corneas of mice with null mutations in lumican (13–17) or keratocan (18, 19) have disclosed specific abnormalities in tissue architecture. Deletions of mimecan, on the other hand, have minimal influence on corneal matrix assembly (20, 21). These observations stimulated several questions that are pivotal to our understanding of the functional roles of the component molecular domains of PGs. To better understand the role of KS sulfation motifs in corneal matrix morphogenesis and uncouple the role of KS GAG from KSPG we investigated the corneas of a newly generated mouse strain with a null mutation in *Chst5*, which encodes a GlcNAc 6-*O*-sulfotransferase that is responsible for the sulfation of KS GAG chains.

## Results

To elucidate the biological functions of sulfated KS GAG in mouse cornea *in vivo*, a target vector was constructed that contained a *Chst5* DNA fragment with a neomycin-resistant gene that substituted the ORF of *Chst5*. Homologous recombinant ES cells were produced (Fig. 1*A*) and used to generate *Chst5*-null mice by intercrossing *Chst5* heterozygotes (Fig. 1*B*). Homozygous mutants did not express *Chst5* mRNA (Fig. 1*C*). Genotyping at 3 weeks of age disclosed that ≈25% of pups were *Chst5*-null. The null mice were normally developed at their embryonic stage and born without any critical deficiencies. Follow-up study after 1 yr showed that *Chst5* mutations were nonlethal and the mice developed normally with no outward signs of abnormal gait or skeletal deformities. On slit-lamp examination corneas were transparent in the homozygous, heterozygous, and WT animals. *Chst5*-null corneas displayed normal tissue stratification on histological examination, but were significantly thinner than normal with a stroma that measured 51.1 ± 4.5 $\mu$m ($n$ = 12) compared with 63.1 ± 4.6 $\mu$m ($n$ = 12) in heterozygous mice ($P < 0.001$) and 66.3 ± 9.0 $\mu$m ($n$ = 16) in WT

Conflict of interest statement: No conflicts declared.

This paper was submitted directly (Track II) to the PNAS office.

Abbreviations: KS, keratan sulfate; CS, chondroitin sulfate; DS, dermatan sulfate; PG, proteoglycan; GAG, glycosaminoglycan.

††To whom correspondence should be addressed. E-mail: knishida@oph.med.tohoku.ac.jp.

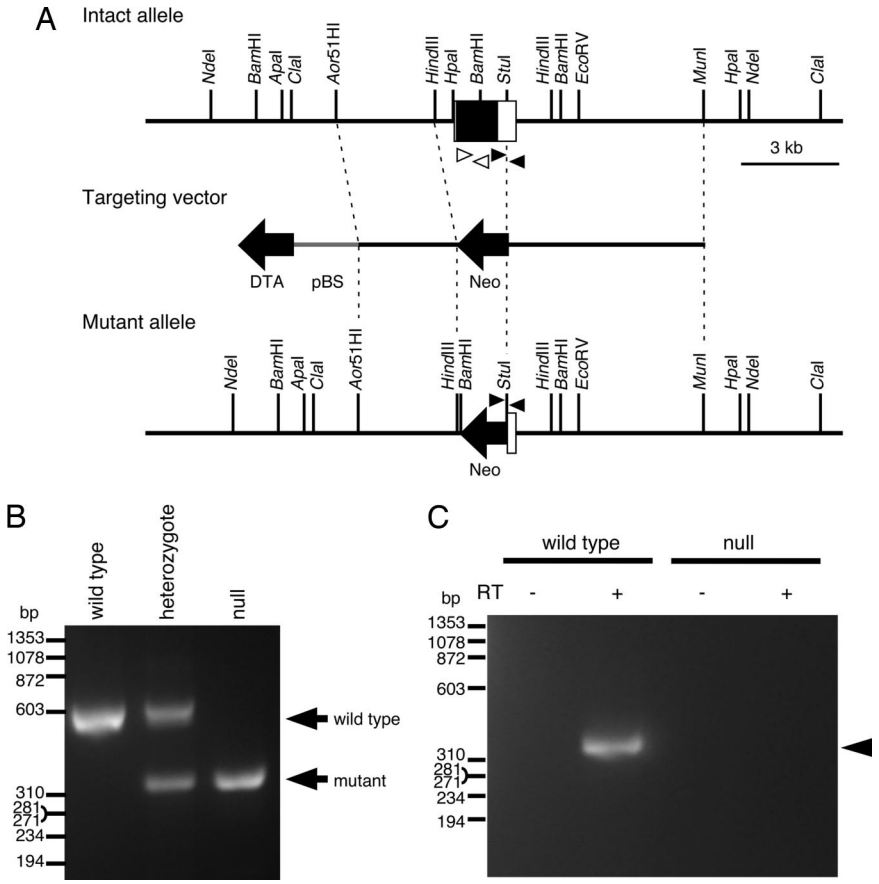


**Fig. 1.** Generation of *Chst5*-null mice. (*A*) Structure of the targeting vector and generated mutant allele. *Chst5* exon 2 (white box) including a single ORF (black box) was replaced with a neomycin-resistant gene (Neo, shown by a black arrow) in the targeting vector and generated mutant allele. The negative selection marker, DTA, and plasmid vector backbone, pBS, are shown by a black arrow and a gray line, respectively. (*B*) Normal and mutant alleles generated by homologous recombination with the targeting vector were detected by genomic PCR analysis using specific primers shown as black arrowheads in *A*. (*C*) RT-PCR analysis using primers indicated as white arrowheads in *A* also confirmed the presence and absence of *Chst5* mRNA (indicated by an arrowhead) in the whole eyes of WT and *Chst5*-null mice, respectively.

mice ($P < 0.001$) (Figs. 2 and 3). Epithelial thickness, as evidenced by the cornea/stroma thickness ratios, was unaffected (Fig. 3).

**PG Composition.** Previously, we found comparatively low levels of sulfated KS in normal mouse cornea based on immunoreactivity with 5D4 (22), a mAb that recognizes high sulfated sequences of residues (minimally penta-sulfated) on poly *N*-acetyllactosamine disaccharides of KS (23, 24). In the current study these KS epitopes were detected in extracts of WT and heterozygous corneas, but not in corneal extracts from homozygous *Chst5*-null mice (Fig. 4).

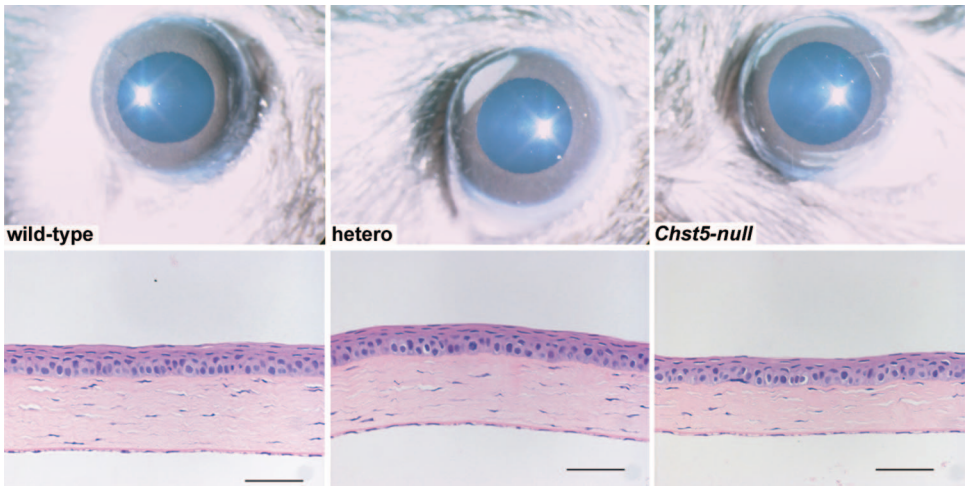


**Fig. 2.** Corneas of WT, heterozygous, and homozygous *Chst5*-null mice with no evidence of tissue opacification. Histologic sections show normal tissue stratification, but with an indication of a relatively thin stroma in the mutant mouse. (Scale bars: 50 $\mu$m.)

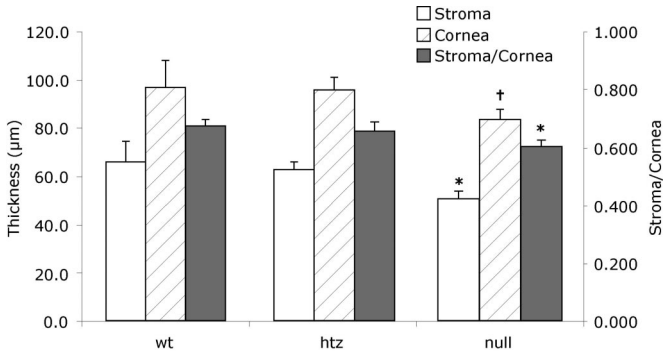


**Fig. 3.** Corneal thickness measured from tissue sections in each genotype group (WT, $n = 12$; heterozygous, $n = 12$; *Chst5*-null, $n = 16$) confirms that a thin stroma is a feature of the *Chst5*-null mouse. Open, hatched, and filled bars indicate stromal thickness, corneal thickness, and the stroma/cornea thickness ratio, respectively. *, $P < 0.001$ for both WT-null and heterozygous-null comparisons. †, $P < 0.003$ for WT-null and $P < 0.001$ for heterozygous-null.

Immunoblot analysis of corneal extracts with a mAb to lumican, however, identifies the presence of KSPG core protein in the corneas of *Chst5*-deficient mice (Fig. 4). On electron microscopy WT corneas that had been incubated in chondroitinase ABC [to digest chondroitin sulfate (CS)/dermatan sulfate (DS) GAG chains] and stained with Cupromeronic blue exhibited sulfated KSPGs as small electron-dense, collagen-associated filaments (Fig. 5). *Chst5*-null corneas, on the other hand, contained no detectable Cupromeronic blue-stained KSPG filaments, indicating their abolishment by the *Chst5* mutation (Fig. 5). As was discovered recently, large chondroitinase ABC-susceptible, Cupromeronic blue-stained PG filaments are a feature of the normal mouse cornea (22). In *Chst5*-null mouse corneas the large PG filaments take on a highly unusual branched "caterpillar-like" morphology (Fig. 5). They are removed from the tissue by incubation in chondroitinase ABC, but not keratanase I, indicating a significant CS/DS component.

**Collagen Matrix Architecture.** In all genotypes, electron microscopy revealed a typical lamellar organization of aligned collagen fibrils

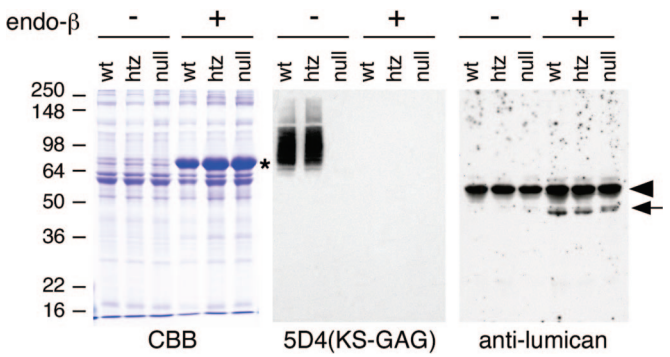


**Fig. 4.** Immunoblot analysis of corneal KSPG. Corneal protein extracts were stained with Coomasie brilliant blue (CBB) (*Left*) and analyzed for the presence of sulfated KS-GAG by 5D4 mAb (*Center*) and the expression of KSPG core protein by antilumican antibody (*Right*). Lanes of corneal protein extracts from *Chst5*-WT, heterozygote, and null mice are indicated as wt, htz, and null, respectively. Each extract was incubated with (+) and without (−) endo-β-galactosidase before SDS/PAGE. A major band found in lanes of endo-β-galactosidase-digested protein on the SDS/PAGE pattern (marked by *) is exogenous BSA included with endo-β-galactosidase as a stabilizer. A prominent band (arrowhead) on the immunoblot with antilumican antibody is endogenous mouse Ig heavy chain detected by the secondary antibody. On 5D4 immunostaining, the *Chst5*-null lane was negative for sulfated KS GAG. Lumican protein (arrow) was detected in endo-β-galactosidase-treated lanes in corneal extracts from all three genotypes.

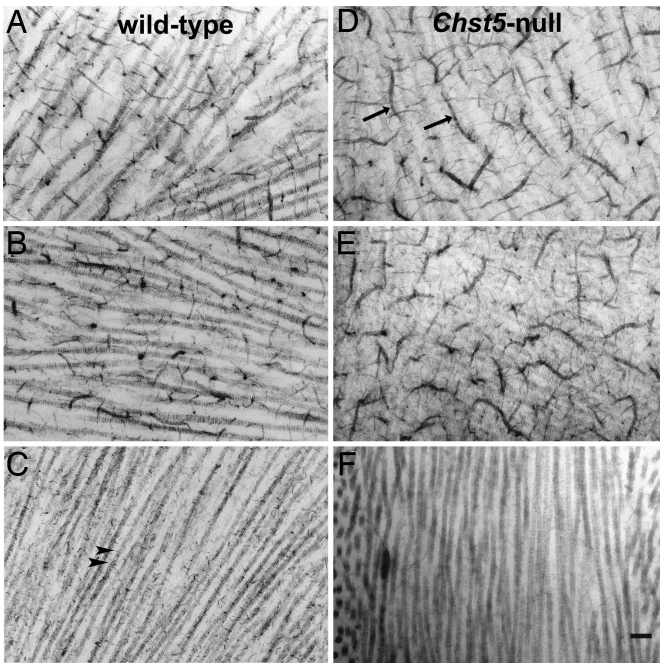


**Fig. 5.** Electron micrographs of the corneal stroma in WT (*Left*) and homozygous *Chst5*-null mice (*Right*), showing PGs stained with Cupromeronic blue after incubation in buffer (*A* and *D*), keratanase (*B* and *E*), and chondroitinase ABC (*C* and *F*). Small collagen-associated PG filaments remaining after chondroitinase ABC digestion in the WT cornea (*C*, arrowheads) represent sulfated KSPGs. These are not present in *Chst5*-null cornea (*F*). Abnormally large, caterpillar-like PGs (arrows), not present in the WT stroma (*A*), are evident in the *Chst5*-null cornea (*D*). These are susceptible to chondroitinase ABC (*F*), but not to keratanase (*E*), digestion pointing to a significant CS/DS component. (Scale bar: 300 nm.)

with uniform diameters and no evidence in *Chst5*-null corneas of the large, fused collagen fibrils that form in the corneas of mice with targeted gene deletions of the major corneal KSPG, lumican (data not shown) (14). To discover whether *Chst5* deletions have a bearing on the overall corneal matrix structure we undertook a series of synchrotron x-ray fiber diffraction experiments. Resultant diffraction patterns produced by corneas of homozygous *Chst5*-null mice were noticeably different from the corresponding diffraction patterns obtained from the corneas of WT or heterozygous mice (Fig. 6). X-ray data were acquired from whole, isolated corneas maintained close to physiologic hydration, and collagen fibrils throughout the whole of the cornea's thickness in the tissue volume through which the x-ray beam passes contribute to the diffraction pattern (25). Thus, sampling is extensive, generating representative measurements of collagen matrix architecture.

Analyses of the x-ray diffraction patterns indicated a marked alteration in the collagen fibrillar ultrastructure in the *Chst5*-null cornea (Table 1). The average diameter of collagen fibrils throughout the whole depth of the corneal stroma in homozygous mice ($34.7 \pm 0.7$ nm; $n = 18$) was marginally, but significantly, lower than the corresponding value for heterozygous ($35.7 \pm 0.6$ nm; $n = 11$; $P < 0.001$) or WT ($36.5 \pm 0.9$ nm; $n = 12$; $P < 0.001$) corneas. The overall spatial arrangement of collagen fibrils in the *Chst5*-null cornea was manifestly different. Diffraction patterns from *Chst5*-null corneas all possessed a first-order equatorial (i.e., interfibrillar) x-ray reflection that was visibly less well defined than the corresponding reflection obtained from WT corneas or heterozygous corneas (Fig. 6). From the angular spread of these reflections a quantity called the coherence distance was calculated according to Regini and associates (26). Described by Stokes (27) as "the average distance over which exact periodicity [of the collagen fibrillar array]

BIOCHEMISTRY

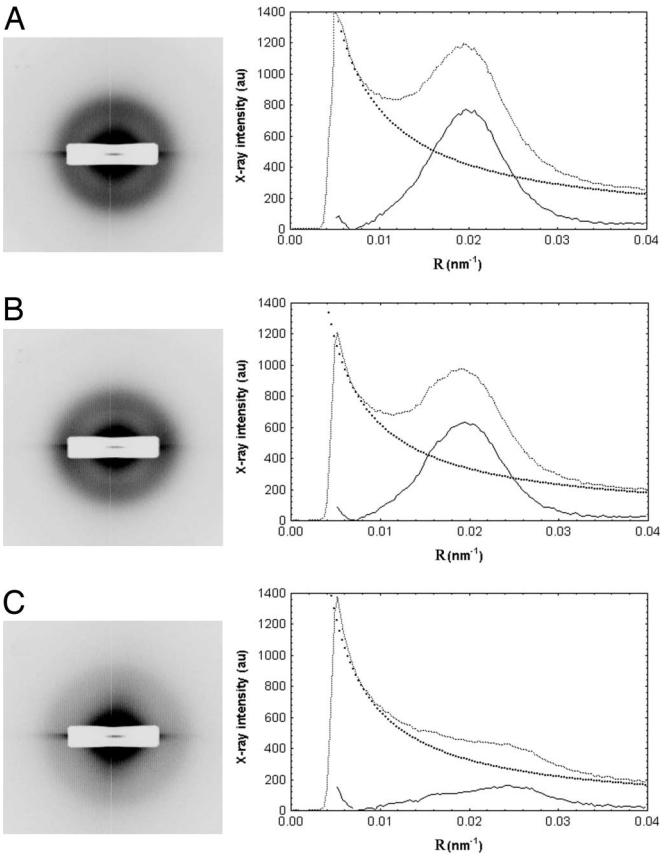


**Fig. 6.** Synchrotron x-ray fiber diffraction patterns from the corneas of WT (*A*), heterozygous (*B*), and homozygous (*C*) *Chst5*-null mice revealing a more diffuse collagen interfibrillar x-ray reflection in the homozygous situation. Background-subtracted peaks in the x-ray intensity profiles from the patterns confirm the diffuseness of the interfibrillar reflection and enable calculation of the mean center-to-center collagen interfibrillar Bragg spacing.

begins to fail," higher coherence distance values are indicative of more local order in the stromal matrix. Values here were found to be lower in corneas of homozygous mutants (184 ± 19 nm; $n = 18$) than heterozygous mutants (236 ± 13 nm; $n = 11$) or WTs (249 ± 17 nm; $n = 12$) (Table 1). Average center-to-center collagen interfibrillar Bragg spacing in the corneas of homozygous *Chst5*-null mice (42.6 ± 3.4 nm; $n = 18$) was discovered to be significantly lower than the corresponding value for WT (47.8 ± 3.5 nm; $n = 12$; $P < 0.001$) or heterozygous corneas (48.3 ± 2.2 nm; $n = 11$; $P < 0.001$) (Table 1).

## Discussion

The production of mice with KSPG-null mutations has facilitated research into the respective and combined functions of these molecules in the control of extracellular matrix morphogenesis (28–30). Broadly stated, of the three KSPGs in cornea, lumican and keratocan are required to maintain collagen fibrils in a specific spatial conformation (13–19). The influence of mimecan, on the other hand, is minimal (21). Recent work has also shown that lumican and keratocan are related PGs, and that lumican has a regulatory influence over the expression of keratocan at the transcriptional level (31). All KSPG-deficient mice studied thus far are gene-targeted mutants that have had the synthesis of a particular KSPG core protein disturbed. To help uncouple the role of KS GAG from KSPG and ascertain the importance of the sulfation of the KS side chains in the governance of matrix ultrastructure, the corneas of a new gene-targeted mouse with *Chst5* mutations were investigated.

**Table 1. Average collagen fibril spacing, diameter, and coherence distances (± SD) in WT, heterozygous, and homozygous *Chst5* corneas**

| Genotype | *n* | Mean collagen fibril Bragg spacing, nm | Mean collagen fibril diameter, nm | Mean coherence distance, nm |
|---|---|---|---|---|
| *Chst5*$^{+/+}$ | 12 | 47.8 ± 3.5 | 36.5 ± 0.9 | 249.3 ± 17.2 |
| *Chst5*$^{+/-}$ | 11 | 48.3 ± 2.2 | 35.7 ± 0.6 | 236.0 ± 12.7 |
| *Chst5*$^{-/-}$ | 18 | 42.6 ± 3.4* | 34.7 ± 0.7* | 184.2 ± 19.2* |

*, $P < 0.001$ for both WT-null and heterozygote-null comparisons.

*Chst5* encodes intestinal GlcNAc 6-*O*-sulfotransferase, a carbohydrate sulfotransferase that is expressed in the intestine and cornea in mouse (4, 32), and which acts on transferring sulfate onto the 6-*O* position of the nonreducing terminal GlcNAc on KS (4). This sulfation step is coupled with the elongation of the KS backbone (33, 34). Sulfation at the 6-*O* position on the galactose residue may depend on the sulfation of GlcNAc (35, 36), thus it can be appreciated how an absence of sulfotransferase activity results in the production of no or extremely low sulfated KS in *Chst5*-null mice. It may also be possible that elongation of the KS backbone is disturbed in the *Chst5*-null cornea because of dramatic loss of hydrophilic residues on the carbohydrate. It is not known whether the absence of GlcNAc sulfation affects the KS chain elongation step in the corneas of homozygous *Chst5*-null mice. Nevertheless, it is now established that, although the tissue continues to express the major corneal KSPG core protein, lumican, it lacks both immunodetectable epitopes of high sulfated KS GAG sequences and histochemically identifiable sulfated KSPG filaments.

The large, caterpillar-like CS/DS PG filaments discovered in the stroma of *Chst5*-deficient corneas on Cupromeronic blue staining appear specific to this tissue. Previous investigations of human corneas have reported an oversulfation of CS/DS PGs in macular corneal dystrophy and suggested that the lack of KS sulfation might lead to an oversulfation of CS/DS (37, 38). It is also possible that the inability to sulfate KS GAG in the *Chst5*-null mouse cornea might result in a compensatory oversulfation of CS/DS and the resultant appearance of chondroitinase ABC-susceptible, caterpillar-like staining complexes.

*In vitro* work by Rada and associates (39) has demonstrated that the fibrillogenesis of corneal collagen is regulated by intact lumican PGs, but that it is equally regulated by lumican core protein alone. The current analysis of isolated whole corneas shows marginally thinner fibrils, on average, in the *Chst5*-null situation, indicating that the sulfation of KS side chains is not a major requirement for the inhibition of collagen fibril growth in the cornea *in situ*. Electron microscopy of *Chst5*-deficient corneas, moreover, found none of the isolated, fused collagen fibrils that are a consistent feature of the lumican-deficient mouse cornea (14). Thus, we conclude that lumican is required to prevent the fusion of collagen fibrils in the corneal stroma, but that this function can be met whether or not the PG is modified with sulfated KS side chains.

The foremost structural change seen in corneas of homozygous *Chst5*-null mice is the abnormally close collagen fibrillar packing (Table 1). *Chst5* is a murine ortholog of *CHST6*, the carbohydrate sulfotransferase gene that in humans is causative for macular corneal dystrophy (10). Interestingly, the human genome has an additional sulfotransferase gene, *CHST5*, as an ortholog for *Chst5* in mouse (4, 10, 32). Because of their high homology, *CHST5* and *CHST6* seem to be created by gene duplication during evolution (10). The coding sequences of the three human and mouse genes are highly homologous, and all of the gene products have sulfotransferase activity over nonreducing terminal GlcNAc (4, 40). Nevertheless, only the enzymes encoded on *CHST6* and *Chst5* have similar substrate specificity and the ability to produce sulfated KS

*in vitro* (4). Thus, in mouse, *Chst5* is the biologically equivalent gene for *CHST6* in humans, and a knockout of *Chst5* in mouse represents a lack of functional *CHST6* in humans. *CHST6* mutations are found in the genomes of macular corneal dystrophy patients throughout the world (10, 41–50), and in the few human corneas that have been examined postoperatively by x-ray fiber diffraction, collagen fibrils are, on average, normal in diameter but are more closely spaced (51). We contend that collagen matrix compaction in the *Chst5*-null mouse is a direct consequence of KS undersulfation. The mechanism by which this matrix compaction occurs is not fully understood, but possibilities include a lower $SO_4^-$ charge repulsion throughout the extrafibrillar space or a lessening of the hydrophilic nature of the corneal stroma.

A structural phenotype in *Chst5*-null corneas is manifest in changed KS (and CS/DS) sulfation patterns, a thin stroma, and altered matrix ultrastructure. As stated, maintenance of the characteristic stromal architecture is believed to be responsible for corneal transparency (12). However, the corneas of homozygous *Chst5*-null mice examined here show no obvious signs of transparency loss. Corneal transparency theory tells us that the fraction of light transmitted through the extracellular corneal matrix, $F(\lambda)$, falls off exponentially with the product of the total scattering cross-section ($\sigma$), the collagen fibril number density ($\rho$), and the thickness of the tissue ($t$), and takes the form $F(\lambda) = e^{-\sigma\rho t}$ (12). A full, quantitative assessment of corneal transparency is a significant task because $\sigma$ is itself a complex function of the wavelength of light, the diameters of the collagen fibrils, their mode of packing, and the ratio of the refractive index of the hydrated fibrils to the refractive index of the extrafibrillar matrix. Nevertheless, we can reason that the decreased interfibrillar spacing found in *Chst5*-null corneas is indicative of a higher $\rho$ value. We conclude, therefore, that the absence of clinically detectable transparency loss in homozygous *Chst5*-null corneas must be caused by the combined effects of the thin stroma in these animals (i.e., reduced $t$), possibly augmented by changes in stromal architecture that lead to a lower $\sigma$ value.

In summary, mutations on *Chst5* result in the undersulfation of KS GAG in murine cornea, the loss of collagen-associated KSPG filaments, and the altered sulfation of CS/DS. Collagen matrix changes also occur in homozygous *Chst5*-null corneas, identifying the sulfation step in KS GAG biosynthesis as a fundamental requirement for tissue morphogenesis.

## Materials and Methods

**Generation of *Chst5*-Null Mice.** To construct the targeting vector, a mouse genomic P1 clone (VJ129 strain) containing *Chst5* was isolated by PCR-based screening. From this screening a 12-kbp DNA fragment, which contained *Chst5* exon 2, was obtained by Aor51H1 and MunI digestion and subcloned into pBluescript II SK vector. The entire ORF of *Chst5* encoded on exon 2 was then replaced with MC1-neo, and diphtheria toxin A subunit sequence was added at the 5′ region of *Chst5*. The constructed targeting vector DNA was linearized with SalI and used to transfect a 129-derived mouse ES cell line. Homologous recombinant ES cells were used to produce chimeric and heterozygote mutant mice. Obtained heterozygotes were subsequently backcrossed to C57BL/6 mice for five to eight generations, after which the mice were intercrossed to obtain null mutants. Genotyping of WT and mutant alleles was performed by PCR analysis using three primers, Ch5WTF1 (5′-GCTGCTGGGTTACCGGTCTGTGCATT-3′), a specific forward primer for intact allele, Ch5KOF2 (5′-GACCGCGCCGCCCCGAC-3′), a specific forward primer for mutant allele, and Ch5R1 (5′-CAGCCCACAGCCGCGCCTTT-3′), a reverse primer for both alleles. Amplification reactions were carried out in a AB2720 Thermal Cycler (Applied Biosystems, Foster City, CA) by 5-min denaturation at 96°C before cycling, 35 cycles of denaturation at 96°C for 30 s, annealing at 66°C for 30 s, extension at 72°C for 30 s, and further extension at 72°C for 5 min.

To confirm expression of *Chst5* transcripts, RT-PCR was performed as follows. Twelve whole eyes were obtained, and total RNA was extracted by using TRIzol reagent (Invitrogen, Carlsbad, CA) according to the manufacturer's instruction. Five micrograms of total RNA was reverse-transcribed by SuperScript II (Invitrogen) and oligo(dT)$_{12–18}$ primer, and an aliquot of the resulted cDNA mixture was examined by PCR analysis using mIGn6RTF primer (5′-GCAGAAGCGCAGCGGGCAG-3′) and mIGn6RTR primer (5′-GTCACGCACGGCCATGTGGAG-3′). The reaction conditions were as described above, except for the use of 45 cycles.

**Light and Electron Microscopy.** Excised eyes of 20 mice (6 WT, 6 heterozygous, and 8 mutant) were fixed in 4% paraformaldehyde and embedded in paraffin. Sections were taken through the central corneas of all 40 eyes, and after staining with hematoxylin and eosin, measurements were made of corneal thickness, stromal thickness, and the corneal/stromal thickness ratio. For electron microscopy excised corneas were fixed in 2.5% glutaraldehyde in 25 mM sodium acetate buffer with Cupromeronic blue (Europa Bioproducts, Cambridge, U.K.) included in the fixative at 0.01% (wt/vol) to stain sulfated PGs in a critical electrolyte concentration mode competing with $MgCl_2$ at 0.1 M (22). Before this process some corneas were incubated in either keratanase I (MP Biomedicals, Costa Mesa, CA; 1 unit/ml in Tris-acetate buffer at pH 8.0) to degrade KS, or chondroitinase ABC (Sigma, St. Louis, MO; 2.5 units/ml in Tris-acetate buffer at pH 7.4), to degrade 0-, 4- and 6-sulfated CS and DS in line with published protocols (22, 38). Ultrathin (silver/gold) sections were stained with 1% aqueous phosphotungstic acid and 0.5% aqueous uranyl acetate (40°C for 40 min in both cases) before examination in a Philips (Eindhoven, The Netherlands) EM208 transmission electron microscope at ×32,000 magnification.

**Immunoblot Analysis of Corneal Protein Extracts.** Twenty mouse corneas were collected into a 1.5-ml microcentrifuge tube and homogenized in 1 ml of guanidine·HCl buffer (4 M guanidine·HCl/50 mM Tris·HCl, pH 8.0/10 mM EDTA, pH 8.0/1 mM PMSF) containing 2 $\mu$l of Protease Inhibitor Mixture (Sigma-Aldrich, St. Louis, MO), using a metal blade homogenizer. The homogenate was shaken at 4°C overnight, and the supernatant was separated by centrifugation and collected. The remaining precipitate was again extracted with 1 ml of guanidine·HCl buffer by shaking at 4°C overnight, and the supernatants were combined. They were then dialyzed against urea buffer (6 M urea/50 mM Tris·HCl, pH 6.8) at 4°C for 24 h, and the resultant solution was recovered in a microcentrifuge tube. After measurement of protein concentration, the solution was adjusted to 1 $\mu$g protein/$\mu$l concentration by urea buffer and stored at −20°C until its use as corneal protein extract for the following experiments.

Twenty micrograms of corneal protein extract was incubated for 12 h at 37°C with or without 1 unit of endo-$\beta$-galactosidase (Associates of Cape Cod, East Falmouth, MA) in 300 $\mu$l of 50 mM sodium acetate, pH 6.5, containing 2 $\mu$l of Protease Inhibitor Mixture. This reaction was stopped by acetone precipitation, after which the resultant protein precipitate was dissolved into 20 $\mu$l of SDS/PAGE sample buffer and subjected to SDS/PAGE. After electrophoresis, separated proteins were either visualized by CBB-R250 staining or transferred onto a PVDF membrane for immunoblotting. For detection of sulfated KS GAG, the filter was blocked with 10% skim milk in PBST5.3 (PBS-0.05% Tween 20, pH 5.3, adjusted with HCl) at room temperature for 1.5 h, and then reacted with diluted 5D4 antibody (Associates of Cape Cod) in 10% skim milk-PBST5.3 for 1 h. The filter was then washed three times with PBST5.3 and reacted with diluted HRP-labeled anti-mouse Ig antibody (Pierce Biotech, Rockford, IL) in 0.3% skim milk-PBST5.3 for 1 h. After washing three times with PBST5.3, the filter was reacted with SuperSignal West Pico chemiluminescent substrate (Pierce Biotech) for 5 min followed by exposure to an x-ray film. For detection of lumican KSPG core protein, the blotted filter

was blocked with 5% BSA in PBST (PBS-0.05% Tween 20) for 1.5 h at room temperature and reacted with diluted mouse monoclonal antilumican antibody in 5% BSA-PBST for 1 h. The filter was then washed three times with PBST followed by incubation with HRP-labeled anti-mouse Ig antibody in 0.3% BSA-PBST for 1 h. After washing three times with PBST, detected signals were visualized as described above.

**Synchrotron X-Ray Fiber Diffraction.** Corneas from 21 mice (9 homozygous mutants, 6 heterozygous mutants, and 6 WTs) were excised at the limbus immediately after death and individually wrapped in Clingfilm to limit dehydration. Specimens were then frozen in dry ice and stored at −80°C before examination by x-ray diffraction at the Synchrotron Radiation Source (SRS), Daresbury Laboratory, Cheshire, U.K (25). Freezing is an accepted way of storing corneas for investigations of matrix structure by synchrotron x-ray scattering (52). For data collection corneas were, in turn, individually secured in a sealed specimen holder between two sheets of Mylar and positioned in the path of the x-ray beam on SRS Station 2.1, such that when the shutters were opened (3-min exposures were used) monochromatic radiation of wavelength 0.154 nm focused to 1.5 × 1.0 mm at the specimen passed through the full thickness of the cornea. Camera length was 9 meters, and fiber diffraction patterns were recorded on a multiwire, gas proportional area detector. Initial data handling using purpose-written, Unix-based software and graphics/statistics packages (Statistica; Statsoft, Tulsa, OK) consisted of normalization with ion chamber counts to correct for beam intensity decay, followed by the subtraction of a detector response from a 14-h exposure to a $Fe^{55}$ radioactive source to correct for any nonlinearities in the detector. X-ray intensity profiles across each diffraction pattern were generated by taking a vertical scan, 26 pixels wide, of x-ray intensity ($I$) versus radial position ($r$). The symmetrical diffraction pattern was then summed about its center to improve the signal-to-noise ratio. As a result the x-ray intensity scans shown in Fig. 6 represent the first-order equatorial $x$-reflection as a single peak plotted against $R$, the reciprocal space coordinate. The average center-to-center collagen interfibrillar Bragg spacing and average collagen fibril diameter were calculated, respectively, from the positions of the first-order equatorial x-ray reflection and the position of the first subsidiary maximum as described by Meek and Quantock (25). The angular width of the first-order equatorial (i.e., interfibrillar) reflection was used to obtain an appreciation of the degree of local order in the fibrillar array by calculating the coherence distance as described by Regini and associates (26).

We thank Dr. Gunter Grossmann and staff at the Synchrotron Radiation Source for help with data collection and the Central Laboratory of the Research Councils for beamtime at the Synchrotron Radiation Source (K.M.M. and A.J.Q.). This work was supported by Biotechnology and Biological Sciences Research Council Project Grant 72/B18021 (to A.J.Q. and B.C.), National Institutes of Health Grants CA071932 (to M.N.F.) and EY014620 (to T.O.A.), Medical Research Council Program Grant G0001033 (to K.M.M., B.C., and A.J.Q.), and the Arthritis Research Campaign U.K.

1. Blochberger, T. C., Vergnes, J.-P., Hempel, J. & Hassell, J. R. (1992) *J. Biol. Chem.* **267,** 347–352.
2. Corpuz, L. M., Funderburgh, J. L., Funderburgh, M. L., Bottomley, G. S., Prakash, S. & Conrad, G. W. (1996) *J. Biol. Chem.* **271,** 9759–9763.
3. Funderburgh, J. L., Corpuz, L. M., Roth, M. R., Funderburgh, M. L., Tasheva, E. S. & Conrad, G. W. (1997) *J. Biol. Chem.* **272,** 28089–28095.
4. Akama, T. O., Nakayama, J., Nishida, K., Hiraoka, N., Suzuki, M., McAuliffe, J., Hindsgaul, O., Fukuda, M. & Fukuda, M. N. (2001) *J. Biol. Chem.* **276,** 16271–16278.
5. Cornuet, P. K., Blochberger, T. C. & Hassell, J. R. (1994) *Invest. Ophthalmol. Visual Sci.* **35,** 870–877.
6. Connon, C. J., Meek, K. M., Kinoshita, S. & Quantock, A. J. (2004) *Exp. Eye Res.* **78,** 909–915.
7. Funderburgh, J. L., Cintron, C., Covington, H. I. & Conrad, G. W. (1988) *Invest. Ophthalmol. Visual Sci.* **29,** 1116–1124.
8. Cintron, C., Gregory, J. D., Dalme, S. P. & Kublin, C. L. (1990) *Invest. Ophthalmol. Visual Sci.* **31,** 1975–1981.
9. Hassell, J. R, Newsome, D. A., Krachmer, J. H. & Rodrigues, M. M. (1980) *Proc. Natl. Acad. Sci. USA* **77,** 3705–3709.
10. Akama, T. O., Nishida, K., Nakayama, J., Watanabe, H., Ozaki, K., Nakamura, T., Dota, A., Kawasaki, S., Inoue, Y., Maeda, N., *et al.* (2000) *Nat. Genet.* **26,** 237–241.
11. Komai, Y. & Ushiki, T. (1991) *Invest. Ophthalmol. Visual Sci.* **32,** 2244–2258.
12. Farrell, R. A. (1994) in *Principles and Practice of Ophthalmology*, eds. Albert, D. M. & Jacobiec, S. A. (Saunders, Philadelphia), pp. 64–81.
13. Chakravarti, S., Magnuson, T., Lass, J. H., Jepsen, K. J., LaMantia, C. & Carroll, H. (1998) *J. Cell Biol.* **141,** 1277–1286.
14. Chakravarti, S., Petroll, W. M., Hassell, J. R., Jester, J. V., Lass, J. H., Paul, J. & Birk, D. E. (2000) *Invest. Ophthalmol. Visual Sci.* **41,** 3365–3373.
15. Quantock, A. J, Meek, K. M. & Chakravarti, S. (2001) *Invest. Ophthalmol. Visual Sci.* **42,** 1750–1756.
16. Song, J., Lee, Y.-G., Houston, J., Petroll, W. A. Chakravarti, S., Cavanagh, H. D. & Jester, J. V. (2003) *Invest. Ophthalmol. Visual Sci.* **44,** 548–557.
17. Beecher, N., Chakravarti, S., Joyce, S., Meek, K. M. & Quantock. A. J. (2006) *Invest. Ophthalmol. Visual Sci.* **47,** 146–150.
18. Liu, C. Y., Birk, D. E., Hassell, J. R., Kane, B. & Kao, W. W. Y. (2003) *J. Biol. Chem.* **278,** 21672–21677.
19. Meek, K. M., Quantock, A. J., Boote, C., Liu, C. Y. & Kao, W. W. Y. (2003) *Matrix Biol.* **22,** 467–475.
20. Tasheva, E. S., Koester, A., Paulson, A. Q., Garrett, A. S., Boyle, D. L., Davidson, H. J., Song, M., Fox, N. & Conrad, G. W. (2002) *Mol. Vis.* **8,** 407–415.
21. Beecher, N., Carlson, C., Allen, B. R., Kipchumba, R., Conrad, G. W., Meek, K. M. & Quantock, A. J. (2005) *Invest. Ophthalmol. Visual Sci.* **46,** 4046–4049.
22. Young, R. D., Tudor, D., Hayes, A. J., Kerr, B., Hayashida, Y., Nishida, K., Meek, K. M., Caterson, B. & Quantock, A. J. (2005) *Invest. Ophthalmol. Visual Sci.* **46,** 1973–1978.
23. Caterson, B., Christner, J. E. & Baker, J. R. (1983) *J. Biol. Chem.* **258,** 8848–8854.
24. Mehmet, H., Scudder, P., Tang, P. W., Hounsell, E. F., Caterson, B. & Feizi, T. (1986) *Eur. J. Biochem.* **157,** 385–391.
25. Meek, K. M. & Quantock, A. J. (2001) *Prog. Ret. Eye Res.* **20,** 95–137.
26. Regini, J. W., Elliott, G. F. & Hodson, S. A. (2004) *J. Mol. Biol.* **336,** 179–186.
27. Stokes, A. R. (1955) *Prog. Biophys.* **5,** 5–167.
28. Chakravarti, S. (2001) *Exp. Eye Res.* **73,** 411–419.
29. Chakravarti, S. (2002) *Glycoconjugate J.* **19,** 287–293.
30. Kao, W. W. Y. & Liu, C. Y. (2002) *Glycoconjugate J.* **19,** 275–285.
31. Carlson, E. C., Liu, C. Y., Chikama, T. I., Hayashi, Y., Kao, C. W. C., Birk, D. E., Funderburgh, J. L, Jester, J. V. & Kao, W. W. Y. (2005) *J. Biol. Chem.* **280,** 25541–25547.
32. Lee, J. K., Bhakta, S., Rosen, S. D. & Hemmerich, S. (1999) *Biochem. Biophys. Res. Commun.* **263,** 543–549.
33. Funderburgh, J. L. (2000) *Glycobiology* **10,** 951–958.
34. Akama, T. O., Misra, A. K., Hindsgaul, O. & Fukuda, M. N. (2002) *J. Biol. Chem.* **277,** 42505–42513.
35. Fukuta, M., Inazawa, J., Torii, T., Tsuzuki, K., Shimada, E. & Habuchi, O. (1997) *J. Biol. Chem.* **272,** 32321–32328.
36. Torii, T., Fukuta, M. & Habuchi, O. (2000) *Glycobiology* **10,** 203–211.
37. Plaas, A. H., West, L. A., Thonar, E. J.-M. A., Karcioglu, Z. A., Smith, C. J., Klintworth, G. K. & Hascall, V. C. (2001) *J. Biol. Chem.* **276,** 39788–39796.
38. Meek, K. M., Quantock, A. J., Elliott, G. F., Ridgway, A. E. A., Tullo, A. B., Bron, A. J. & Thonar, E. J.-M. A. (1989) *Exp. Eye Res.* **49,** 941–958.
39. Rada, J., Cornuet, P. K. & Hassell, J. R. (1993) *Exp. Eye Res.* **56,** 635–648.
40. Hemmerich, S. & Rosen, S. D. (2000) *Glycobiology* **10,** 849–856.
41. Lui, N.-P., Sew-Knight, S., Rayner, M., Jonasson, F., Akama, T. O., Fukuda, M. N., Bao, W., Gilbert, J. R., Vance, J. M. & Klintworth, G. K. (2000) *Mol. Vis.* **6,** 261–264.
42. El-Ashry, M. F., Abd El-Aziz, M. M., Wilkins, S., Cheetham, M. E., Wilkie, S. E., Hardcastle, A. J., Halford, S., Bayoumi, A. Y., Ficker, L. A., Tuft, S., *et al.* (2002) *Invest. Ophthalmol. Visual Sci.* **43,** 377–382.
43. Iida-Hasegawa, N., Furuhata, A., Hayatsu, H., Murakami, A., Fujiki, K., Nakayasu, K. & Kanai, A. (2003) *Invest. Ophthalmol. Visual Sci.* **44,** 3272–3277.
44. Sultana, A., Sridhar, M. S., Jagannathan, A., Balasubramanian, D., Kannabiran, C. & Klintworth, G. K. (2003) *Mol. Vis.* **9,** 730–734.
45. Warren, J. F., Aldave, A. J., Srinivasan, M., Thonar, E. J., Kumar, A. B., Cevallos, V., Whitcher, J. P. & Margolis, T. P. (2003) *Arch. Ophthalmol.* **121,** 1608–1612.
46. Ha, N. T., Chau, H. M., Cung, L. X., Thanh, T. K., Fujiki, K., Murakami, A., Hiratsuka, Y. & Kanai, A. (2003) *Invest. Ophthalmol. Visual Sci.* **44,** 3310–3316.
47. Ha, N. T., Chau, H. M., Cung, L. X., Kim, T. T., Fujiki, K., Murakami, A., Hiratsuka, Y., Hasegawa, N. & Kanai, A. (2003) *Cornea* **22,** 508–511.
48. Aldave, A. J., Yellore, V. S., Thonar, E. J., Udar, N., Warren, J. F., Yoon, M. K., Cohen, E. J., Rapuano, C. J., Laibson, P. R., Margolis, T. P. & Small, K. (2004) *Am. J. Ophthalmol.* **137,** 465–473.
49. Abbruzzese, C., Kuhn, U., Molina, F., Rama, P. & De Luca, M. (2004) *Clin. Genet.* **65,** 120–125.
50. El-Ashry, M. F., Abd El-Aziz, M. M., Shalaby, O., Wilkins, S., Poopalasundaram, S., Cheetham, M., Tuft, S. J., Hardcastle, A. J., Bhattacharya, S. S. & Ebenezer, N. D. (2005) *Am. J. Ophthalmol.* **139,** 192–193.
51. Quantock, A. J., Meek, K. M., Ridgway, A. E. A., Bron, A. J. & Thonar, E. J.-M. A. (1990) *Curr. Eye Res.* **9,** 393–398.
52. Fullwood, N. J. & Meek, K. M. (1994) *J. Mol. Biol.* **236,** 749–758.